

Characterizing entanglement in non-Hermitian chaotic systems via out-of-time ordered correlators

Kai-Qian Huang(黄恺芊), Wei-Lin Li(李蔚琳), Wen-Lei Zhao(赵文垒), and Zhi Li(李志)
Citation: Chin. Phys. B, 2022, 31 (**9**): 090301. DOI: 10.1088/1674-1056/ac67c3
Journal homepage: http://cpb.iphy.ac.cn; http://iopscience.iop.org/cpb

What follows is a list of articles you may be interested in

Effects of colored noise on the dynamics of quantum entanglement of a one-parameter qubit—qutrit system

Odette Melachio Tiokang, Fridolin Nya Tchangnwa, Jaures Diffo Tchinda,Arthur Tsamouo Tsokeng, and Martin Tchoffo
Chin. Phys. B, 2022, 31 (**5**): 050306. DOI: 10.1088/1674-1056/ac2f36

Influences of spin-orbit interaction on quantum speed limit and entanglement of spin qubits in coupled quantum dots

M Bagheri Harouni
Chin. Phys. B, 2021, 30 (**9**): 090301. DOI: 10.1088/1674-1056/abeef4

Nonlocal advantage of quantum coherence and entanglement of two spins under intrinsic decoherence

Bao-Min Li(李保民), Ming-Liang Hu(胡明亮), and Heng Fan(范桁)
Chin. Phys. B, 2021, 30 (**7**): 070307. DOI: 10.1088/1674-1056/abff2a

Entanglement properties of GHZ and W superposition state and its decayed states

Xin-Feng Jin(金鑫锋), Li-Zhen Jiang(蒋丽珍), and Xiao-Yu Chen(陈小余)
Chin. Phys. B, 2021, 30 (**6**): 060301. DOI: 10.1088/1674-1056/abd74e

Quantifying entanglement in terms of an operational way

Deng-Hui Yu(于登辉) and Chang-Shui Yu(于长水)
Chin. Phys. B, 2021, 30 (**2**): 020302. DOI: 10.1088/1674-1056/abc157

Characterizing entanglement in non-Hermitian chaotic systems via out-of-time ordered correlators

Kai-Qian Huang(黄恺芊)[1], Wei-Lin Li(李蔚琳)[1], Wen-Lei Zhao(赵文垒)[2,†], and Zhi Li(李志)[1,3,4,‡]

[1] *Guangdong Provincial Key Laboratory of Quantum Engineering and Quantum Materials, SPTE, South China Normal University, Guangzhou* 510006, *China*
[2] *School of Science, Jiangxi University of Science and Technology, Ganzhou* 341000, *China*
[3] *Guangdong-Hong Kong Joint Laboratory of Quantum Matter, Frontier Research Institute for Physics, South China Normal University, Guangzhou* 510006, *China*
[4] *Guangdong Provincial Key Laboratory of Nuclear Science, Institute of Quantum Matter, South China Normal University, Guangzhou* 510006, *China*

(Received 17 February 2022; revised manuscript received 6 April 2022; accepted manuscript online 18 April 2022)

We investigate the quantum entanglement in a non-Hermitian kicking system. In the Hermitian case, the out-of-time ordered correlators (OTOCs) exhibit the unbounded power-law increase with time. Correspondingly, the linear entropy, which is a common measurement of entanglement, rapidly increases from zero to almost unity, indicating the formation of quantum entanglement. For strong enough non-Hermitian driving, both the OTOCs and linear entropy rapidly saturate as time evolves. Interestingly, with the increase of non-Hermitian kicking strength, the long-time averaged value of both OTOCs and linear entropy has the same transition point where they exhibit the sharp decrease from a plateau, demonstrating the disentanglment. We reveal the mechanism of disentanglement with the extension of Floquet theory to non-Hermitian systems.

Keywords: out-of-time ordered correlators, quantum entanglement, non-Hermiticity

PACS: 03.65.–w **DOI:** 10.1088/1674-1056/ac67c3

1. Introduction

Out-of-time ordered correlators (OTOCs), $C(t) = -\langle [A(t),B]^2\rangle$, have attracted extensive investigations in the field of gravity physics,[1–3] quantum chaos[4–6] and quantum information.[7–9] Growth of OTOCs characterizes the spread of local information over many degrees of freedom. For chaotic systems, OTOCs exhibit exponential dependence on time with growth rate being determined by the Lyapunov exponent.[1] In addition, OTOCs constitute a robust alternative to measure information scrambling, as it can be detected by nuclear magnetic resonance systems.[10] More importantly, since OTOCs are related to the second Rényi entropy[11–13] and quantum Fisher information,[10] quantum entanglement can be indirectly reflected by the measurement of OTOCs.

Non-Hermitian physics has been accepted as a complement of traditional quantum physics. In has been found that Hamiltonian with parity–time ($\mathcal{PT}$) symmetry owns real eigenspectra.[14–16] Such a fascinating feature motivates research in optical waveguides,[17–27] cold atom systems,[28–32] Floquet systems,[32–42] etc. In particular, a lot of exotic phenomena have been found in kicking systems (systems subject to periodical pulses) with $\mathcal{PT}$-symmetry. For example, the quantum state of a $\mathcal{PT}$ kicked particle will evolve to one of the localized quasieigenstate (QES) with complex quasieigenvalue (QEV).[37] This localization can be destroyed by nonlinearity-induced self-interaction, which leads to superexponential growth of the mean energy, i.e., $\langle p^2\rangle = \exp[\exp(\alpha t+\beta)]$.[40] Interestingly, the non-Hermitian kicking potential can protect the quantum coherence in chaotic systems since the quantum state evolves to the localized QES with maximum imaginary part of the QEV.[41] Recent investigation has reported the quantized response of OTOCs to the $\mathcal{PT}$ symmetric kicking potential.[42]

So far, the characterization of the entanglement with OTOCs in non-Hermitian systems is still an open problem. In this work, we investigate it via a bipartite system with $\mathcal{PT}$-symmetric kicking potential. We find that, in the Hermitian case, the OTOCs increase in a power law of time. Intriguingly, when the non-Hermitian driving strength is strong enough, the growth of OTOCs is suppressed and the freezing of OTOCs occurs. The linear entropy increases from zero to almost unity with time in the Hermitian case, which indicates entanglement production. However, the non-Hermitian driving can effectively suppress the growth of linear entropy. We further investigate the long-time averaged value of both OTOCs and linear entropy. Our result shows that there is a turning point where both the time-averaged OTOCs and linear entropy exhibit a sharp decrease from the plateau, thus the occurrence of disentanglment is demonstrated. More interestingly, the transition point is in the vicinity of the $\mathcal{PT}$-symmetric breaking point. The paper is organized as follows. In Section 2, we present the model. Section 3 shows the result of the OTOCs and entangle-

[†]Corresponding author. E-mail: wlzhao@jxust.edu.cn
[‡]Corresponding author. E-mail: lizphys@m.scnu.edu.cn

© 2022 Chinese Physical Society and IOP Publishing Ltd

ment. The physics mechanism is given in Section 4. Summary is presented in Section 5.

2. Model

The Hamiltonian of the bipartite system reads

$$H = H_1 + H_2 + H_{\rm I}, \tag{1}$$

where H_j ($j = 1,2$) represents the Hamiltonian of an individual particle, and $H_{\rm I}$ is the interaction. Each subsystem is a kicked particle within an infinite square well, whose Hamiltonian takes the form

$$H_j = \frac{{p_j}^2}{2} + V(x_j) + V_{\rm K}(x_j)\sum_n \delta(t-n), \tag{2}$$

with

$$V(x_j) = \begin{cases} 0, & \text{if } |x_j| < \frac{L}{2}, \\ +\infty, & \text{otherwise}, \end{cases} \tag{3}$$

and the potential with $\mathcal{PT}$-symmetry reads

$$V_{\rm K}(x_j) = K_j[\cos(x_j) + {\rm i}\lambda_j \sin(x_j)], \tag{4}$$

where $p_j = m_j \pi \hbar_{\rm eff}/L$ with m_j ($\hbar_{\rm eff}$ and L) being the quantum number of energy (the effective Plank constant and the width of potential well). In addition, x_j (K_j and λ_j) denotes the coordinate (the kicking strength and the non-Hermitian parameter). The interaction Hamiltonian reads

$$H_{\rm I} = \mu \cos(x_1)\cos(x_2)\sum_n \delta(t-n), \tag{5}$$

with μ being the interaction strength. The Schrödinger equation of the bipartite system in dimensionless unites is written as

$${\rm i}\hbar_{\rm eff}\frac{\partial \psi}{\partial t} = H\psi. \tag{6}$$

The time evolution from $t = n$ to $t = n+1$ is governed by the Floquet operator $|\psi(n+1)\rangle = U|\psi(n)\rangle$. Due to the δ-kick, the Floquet operator U can be divided into two parts

$$U = U_{\rm f} U_{\rm K}, \tag{7}$$

where the evolution operator of the kinetic term is expressed as

$$U_{\rm f} = \exp\left(-\frac{\rm i}{\hbar_{\rm eff}}\sum_j \frac{p_j^2}{2}\right), \tag{8}$$

and for the kick term, it is

$$U_{\rm K} = \exp\left[-\frac{\rm i}{\hbar_{\rm eff}}\sum_j V_{\rm K}(x_j) - \frac{\rm i}{\hbar_{\rm eff}} H_{\rm I}(x_1,x_2)\right]. \tag{9}$$

For simplicity, we consider the case that the two particles are identical, i.e., $K_1 = K_2 = K$ and $\lambda_1 = \lambda_2 = \lambda$. In fact, we have investigated the case that $\lambda_1 = 0$ and λ_2 varies. There is no essential difference between the two cases. In numerical simulation, we set the initial state as the product state of the ground state $\psi(x_1,x_2,0) = 2\cos(\pi x_1/L)\cos(\pi x_2/L)/L$.

3. Characterizing entanglement with OTOCs

3.1. OTOCs dynamics

The OTOCs are defined by $C(t) = -\langle[A(t),B]^2\rangle$, where the operator $A(t)$ in Heisenberg picture reads $A(t) = U^\dagger(t)AU(t)$. When both A and B are in the same subsystem, i.e., $(A = p_1^2, B = p_1^2)$ with $C_{11} = -\langle[p_1^2(t), p_1^2]^2\rangle$, the OTOCs can demonstrate intrasubsystem scrambling. If A and B are in different subsystems, i.e., $(A = p_1^2, B = p_2^2)$ with $C_{12} = -\langle[p_1^2(t), p_2^2]^2\rangle$, the OTOCs can quantify intersubsystem scrambling.[3] There have been many reports on the Hermitian systems (i.e., $\lambda = 0$) proved that the two-particle interaction can destroy the quantum coherence if the interaction is strong enough.[43–52] As a consequence, the quantum diffusion is in consistence with its classical counterpart, i.e., the quantum-classical correspondence (QCC), and the system is chaotic.[41] As for the OTOCs in the Hermitian case, both C_{11} and C_{12} increase in a power law of time, i.e., $C_{11} \propto t^4$ and $C_{12} \propto t^4$, which demonstrates the power-law scrambling in chaotic systems. For a modest λ (e.g., $\lambda = 0.01$), the growth of both C_{11} and C_{12} is consistent with that of $\lambda = 0$ for a short time interval, after which they become saturated, indicating that the information scrambling has ceased growing. From Fig. 1, one can find that large λ leads to early cease of the OTOCs' growth as well as its small saturation value.

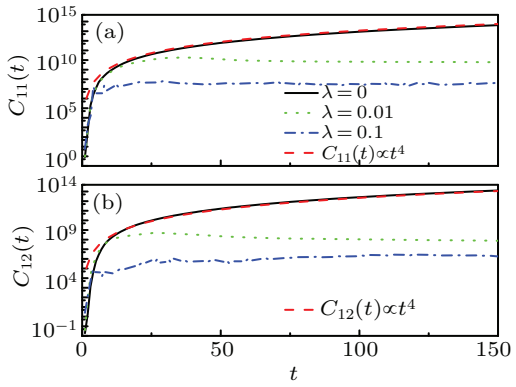


Fig. 1. OTOCs versus time, corresponding to (a) $C_{11} = -\langle[p_1^2(t), p_1^2]^2\rangle$ and (b) $C_{12} = -\langle[p_1^2(t), p_2^2]^2\rangle$. The dashed lines indicate the fitting function of the form $C_{11} \propto t^4$ ($C_{12} \propto t^4$). Other parameters are $K = 5$, $\hbar_{\rm eff} = 0.25$, $\mu = 0.5$, and $L = 2\pi$.

3.2. Entanglement entropy

During the process of QCC, the entanglement between the subsystems grows due to the interaction. To measure the entanglement, we investigate the linear entropy of the system as follows:

$$S(t) = 1 - {\rm Tr}[\rho_1^2(t)]. \tag{10}$$

With the generation of entanglement, a pure state evolves to a mixed one, during which the value of S increases from zero

to almost unity[53,54] [see Fig. 2(a) for $\lambda = 0$]. This process is accompanied by the disappearance of quantum coherence. Therefore, the decoherence effect induced by interaction results in the QCC of diffusion dynamics.

Intriguingly, for a specific λ, the linear entropy increases during the initially short time interval [see Fig. 2(a) for $\lambda = 0.01$], which indicates that the quantum state is a mixed one. After the initial growth, the linear entropy decreases to a saturation value and the quantum state becomes actually a pure state. This clearly demonstrates that the quantum coherence, which is initially destroyed, will partially revive due to the non-Hermitian kicking potential. Therefore, under the effect of non-Hermitian kicking potential, an initially pure state becomes mixed during short time evolution, and eventually evolves to a pure state. This process corresponds to the transition from the decoherence to coherence recovery and entanglement production to disentanglement as time evolves. Note that the decreasing process of the value S to saturation indicates the back flow of information from the environment to the system.[55]

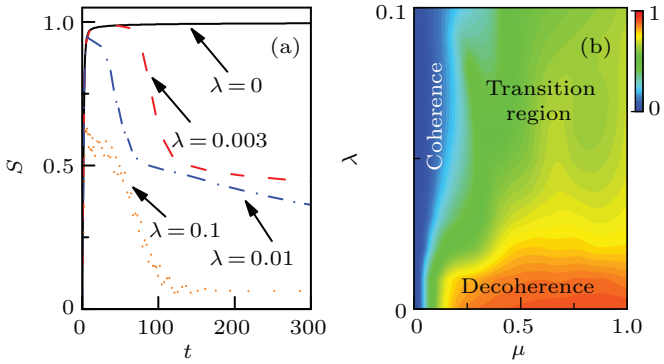


Fig. 2. (a) Linear entropy S versus time with $\mu = 0.5$. (b) The averaged value $\langle S\rangle_t$ in the parameter space (λ, μ). Other parameters are the same as those in Fig. 1.

Moreover, to clearly show the entanglement with different parameters, we further numerically investigate the long-time average of S, i.e.,

$$\langle S\rangle_t = \frac{1}{t_f}\int_0^{t_f} S(t)\,\mathrm{d}t, \tag{11}$$

by varying the interaction strength μ and the non-Hermitian kicking strength λ. Figure 2(b) shows that, for extremely small value of μ, S is almost zero, and the reason is that weak interaction is not enough to thermalize the system.[56] With the increase of interaction, S increases due to the decoherence and quantum entanglement. However, for a certain value of μ, S decreases with large λ. This demonstrates that, though the interaction leads to quantum entanglement and decoherence, the non-Hermitian kicking potential results in the decrease of entanglement and prevents the decoherence, mitigating the effect of interaction.

3.3. Featuring $\mathcal{PT}$-symmetric breaking with OTOCs and linear entropy

When the non-Hermitian kicking potential is weak, the Hamiltonian commutes with the $\mathcal{PT}$ operator, i.e., $[H, \mathcal{PT}] = 0$. The quantum dynamics is similar to that in the Hermitian case and the QEV of the Floquet operator is real [see Eq. (14)]. When the non-Hermitian kicking potential is strong enough, the Hamiltonian does not commute with the $\mathcal{PT}$ operator, i.e., $[H, \mathcal{PT}] \neq 0$ and the $\mathcal{PT}$ symmetry of the Hamiltonian is broken. Some QEVs of the Floquet operator are complex. With appearance of the complex eigenvalue, the norm of the quantum state, $\mathcal{N}$, will grow exponentially with time, rather than unity in the Hermitian case. Thus, the time-averaged value of $\mathcal{N}$, $\langle\mathcal{N}\rangle_t = \frac{1}{t_f}\int_0^{t_f}\mathcal{N}(t)\,\mathrm{d}t$, can help to find the λ_c, the critical value of λ. In Fig. 3(a), we find that as λ increases, $\langle\mathcal{N}\rangle_t$ remains unity and then increases when λ exceeds 10^{-3}, i.e., $\lambda_c \simeq 10^{-3}$.

As discussed above, strong enough non-Hermitian kicking potential can suppress the growth of OTOCs and the saturation value of linear entropy. In order to further quantify the effect of the non-Hermitian kicking potential on the OTOCs and linear entropy, we investigate the time-averaged OTOCs and linear entropy by varying the value of λ. The time-averaged OTOCs $\langle C_{11}\rangle_t$ and $\langle C_{12}\rangle_t$ read

$$\langle C_{11}\rangle_t = \frac{1}{t_f}\int_0^{t_f} C_{11}(t)\,\mathrm{d}t, \tag{12}$$

$$\langle C_{12}\rangle_t = \frac{1}{t_f}\int_0^{t_f} C_{12}(t)\,\mathrm{d}t. \tag{13}$$

Figure 3(b) shows that as the value of λ increases, $\langle C_{11}\rangle_t$ and $\langle C_{12}\rangle_t$ stay at a plateau and then decrease in a power law. Moreover, the turning point is about $\lambda = 10^{-3}$, which is equal to λ_c. This also shows that the QESs with non-zero complex QEVs contribute to the suppression of the OTOCs increase. The discovery that the non-Hermitian kicking potential leads to the saturation of OTOCs opens a new prospect in the field of information scrambling for conventional theory, believing that the many-body localization induces the logarithmic growth of OTOCs.[57]

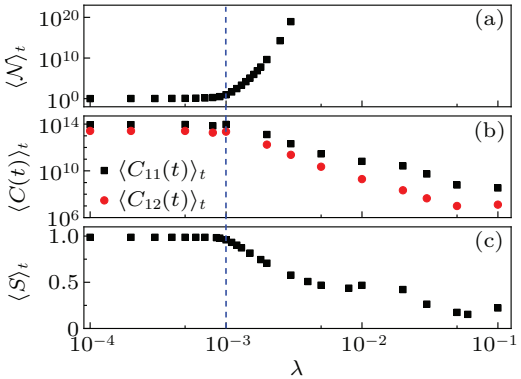


Fig. 3. Dependence of $\langle\mathcal{N}\rangle_t$ (a), $\langle C_{11}\rangle_t$ (squares) and $\langle C_{12}\rangle_t$ (circles) (b), and $\langle S\rangle_t$ (c) on λ. The parameters are the same as those in Fig. 1.

In addition, our numerical results show that the value of S is equal to almost unity for $\langle S\rangle_t$ smaller than a critical value, beyond which the value of $\langle S\rangle_t$ is less than unity, which indicates the coherence recovery and disentanglement. Moreover, it gradually decreases with the increase of λ [see Fig. 3(c)]. This indicates that the appearance of the QES with complex QEV contributes to the recovery of coherence. The recovery will be more salient with stronger non-Hermitian kicking potential, and the saturation of OTOCs decreases with the increase of λ [see Fig. 1]. Thus, the above findings again prove that the OTOCs are closely relevant to entanglement,[9–12,58–66] even in the non-Hermitian case.

4. Physics mechanism

Previous research suggests that in a non-Hermitian system, the inherent physics of the localization of the state is such that the quantum state evolves to one of the eigenstates of the Floquet operator.[37,41] We also investigate the QESs and QEVs of the Floquet operator. The eigenequation of the Floquet operator reads

$$U\varphi_\varepsilon = \mathrm{e}^{-\mathrm{i}\varepsilon}\varphi_\varepsilon, \tag{14}$$

where $|\varphi_\varepsilon\rangle$ is QES and ε is QEV. In the non-Hermitian case, when the $\mathcal{PT}$-symmetry is broken, QEV is a complex number, i.e., $\varepsilon = \varepsilon_\mathrm{r} + \mathrm{i}\varepsilon_\mathrm{i}$. We investigate the fidelity between the dynamically-evolved state, $|\psi(t)\rangle$, and QES takes the form

$$\mathcal{F}(t) = \frac{1}{\mathcal{N}}|\langle\psi(t)|\varphi_\varepsilon\rangle|^2, \tag{15}$$

where $\mathcal{N}$ is the norm of $|\psi(t)\rangle$. The numerical results (Fig. 4) show that the fidelity of most QESs is quite small and only one of them is approximately 1, whose imaginary part of QEV is maximum. This indicates that the dynamically evolved state evolves to the QES with the maximum imaginary part of the QEV. Furthermore, we compare the two states. It can be seen that both of them are localized states and they are in good agreement. All these indicate the reason of the localization such that the quantum state evolves to the localized QES with maximum imaginary part of QEV.

Then let us consider the case of $\lambda > \lambda_\mathrm{c}$. Since interaction will lead to decoherence and entanglement between the two subsystems, both OTOCs and linear entropy increase versus time at the beginning. The corresponding quantum state evolves into a mixed state. However, as time goes by, the effect of non-Hermitian kick gradually becomes apparent. The eigenstate with the maximum imaginary part of the eigenvalue begins to dominate the dynamical behavior of the whole system, where localization has been induced and, simultaneously, the increase of OTOCs and linear entropy has been suppressed. Finally, the two particles disentangle partially, and the quantum state eventually evolves to a pure state.

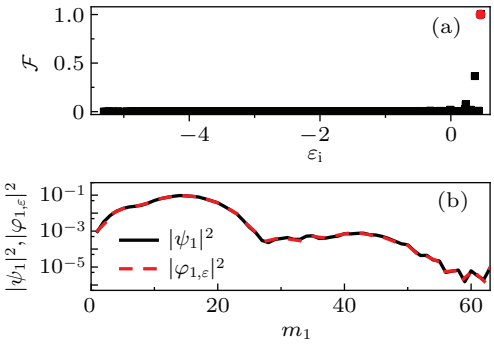


Fig. 4. (a) The fidelity $\mathcal{F}$ between the dynamically-evolved state and the QESs versus the imaginary part of the QEV. The dot marks the QES with $\mathcal{F} \approx 1$. (b) Comparison of the probability density distribution in energy space between the dynamically-evolved state (solid curve) and the QES (dashed curve) with $\mathcal{F} \approx 1$. The parameters are $t = 300$, $\lambda = 0.1$. Other parameters are the same as those in Fig. 1.

5. Summary

We have investigated the quantum entanglement in a bipartite non-Hermitian kicking system. In the Hermitian case, the OTOCs, both C_{11} and C_{12}, exhibit the power-law increase with time. In the non-Hermitian case, the growth of OTOCs can be suppressed by the non-Hermitian kicking potential. The linear entropy increases quickly to unity in the Hermitian case. For strong enough non-Hermitian driving strength, the growth of the linear entropy is suppressed. More importantly, we find that, with the increasing non-Hermitian strength, the long-time averaged values of both OTOCs and linear entropy have the same transition point where they exhibit the sharp decrease from the plateau, demonstrating the disentanglment. This indicates that the OTOC can characterize entanglement. The reason is that there exist localized QESs with complex QEV in the $\mathcal{PT}$-symmetric broken regime. The system will evolve to the localized QES with maximum imaginary part of the QEV, leading to the suppression of the increase of OTOCs and linear entropy. Our work gives an insight into quantum information, quantum communication and other related fields.

Acknowledgements

W. Zhao was supported by the National Natural Science Foundation of China (Grant No. 12065009) and Science and Technology Planning Project of Ganzhou City (Grant No. 202101095077). K. Q. Huang and Z. Li were supported by the National Natural Science Foundation of China (Grant Nos. 11704132, 11874017, and U1830111), the Natural Science Foundation of Guangdong Province, China (Grant No. 2021A1515012350), and the KPST of Guangzhou (Grant No. 201804020055).

References

[1] Maldacena J, Shenker S H and Stanford D 2016 *J. High Energy Phys.* **106** 1
[2] Jahnke V, Kim K Y and Yoon J 2019 *J. High Energy Phys.* **37** 1
[3] Prakash R and Lakshminarayan A 2020 *Phys. Rev. B* **101** 121108

[4] Rozenbaum E B, Ganeshan S and Galitski V 2019 *Phys. Rev. B* **100** 035112
[5] Rozenbaum E B, Bunimovich L A and Galitski V 2020 *Phys. Rev. Lett.* **125** 014101
[6] Wang J Z, Benenti G, Casati G and Wang W G 2020 *Phys. Rev. Res.* **2** 043178
[7] Aleiner I L, Faoro L and Ioffe L B 2016 *Ann. Phys.* **375** 378
[8] Li J, Fan R, Wang H, Ye B, Zeng B, Zhai H, Peng X and Du J 2017 *Phys. Rev. X* **7** 031011
[9] Lewis-Swan R J, Safavi-Naini A, Bollinger J J and Rey A M 2019 *Nat. Commun.* **10** 1581
[10] Gärttner M, Hauke P and Rey A M 2018 *Phys. Rev. Lett.* **120** 040402
[11] Riddell J and Sørensen E S 2019 *Phys. Rev. B* **99** 054205
[12] Fan R, Zhang P, Shen H and Zhai H 2017 *Sci. Bull.* **62** 707
[13] Hosur P, Qi X L, Roberts D A and Yoshida B 2016 *J. High Energy Phys.* **2016** 4
[14] Bender C M and Boettcher S 1998 *Phys. Rev. Lett.* **80** 5243
[15] Bender C M, Boettcher S and Meisinger P N 1999 *J. Math. Phys.* **40** 2201
[16] Bender C M 2007 *Rep. Prog. Phys.* **70** 947
[17] Longhi S 2018 *Europhys. Lett.* **120** 64001
[18] Klaiman S, Günther U and Moiseyev N 2008 *Phys. Rev. Lett.* **101** 080402
[19] Guo A, Salamo G J, Duchesne D, Morandotti R, Volatier-Ravat M, Aimez V, Siviloglou G A and Christodoulides D N 2008 *Phys. Rev. Lett.* **103** 093902
[20] Cartarius H and Wunner G 2012 *Phys. Rev. A* **86** 013612
[21] Rüter C E, Makris K G, El-Ganainy R, Christodoulides D N, Segev M and Kip D 2010 *Nat. Phys.* **6** 192
[22] Ramezani H, Kottos T, El-Ganainy R and Christodoulides D N 2010 *Phys. Rev. A* **82** 043803
[23] Barashenkov I V, Suchkov S V, Sukhorukov A A, Dmitriev S V and Kivshar Y S 2012 *Phys. Rev. A* **86** 053809
[24] Sukhorukov A A, Xu Z and Kivshar Y S 2010 *Phys. Rev. A* **82** 043818
[25] Makris K G, El-Ganainy R, Christodoulides D N and Musslimani Z H 2011 *Int. J. Theor. Phys.* **50** 1019
[26] Benisty H, Degiron A, Lupu A, De Lustrac A, Chénais S, Forget S, Besbes M, Barbillon G, Bruyant A, Blaize S and Lérondel G 2011 *Opt. Express* **19** 18004
[27] Miri M A, Cotrufo M and Alù A 2019 *Opt. Lett.* **44** 3558
[28] Hang C, Gabadadze G and Huang G 2017 *Phys. Rev. A* **95** 023833
[29] Li L, Lee C H and Gong J 2020 *Phys. Rev. Lett.* **124** 250402
[30] Zhang D W, Zhao Y X, Liu R B, Xue Z Y, Zhu S L and Wang Z D 2016 *Phys. Rev. A* **93** 043617
[31] Wang X and Wu J H 2016 *Opt. Express* **24** 4289
[32] Li J, Harter A K, Liu J, de Melo L, Joglekar Y N and Luo L 2019 *Nat. Commun.* **10** 855
[33] Cao Y, Li Y and Yang X 2021 *Phys. Rev. B* **103** 075126
[34] Gong J and Wang Q H 2015 *Phys. Rev. A* **91** 042135
[35] Chitsazi M, Li H, Ellis F M and Kottos T 2017 *Phys. Rev. Lett.* **119** 093901
[36] Harter A K and Joglekar Y N 2020 *Prog. Theor. Experiment. Phys.* **2020** 12A106
[37] Huang K Q, Wang J Z, Zhao W L and Liu J 2021 *J. Phys.: Condens. Matter.* **33** 055402
[38] Zhao W L, Gong P, Wang J and Wang Q 2020 *Chin. Phys. B* **29** 120302
[39] Zhao W L, Wang J, Wang X and Tong P 2020 *Phys. Rev. E* **99** 042201
[40] Zhao W L, Zhou L, Liu J, Tong P and Huang K 2020 *Phys. Rev. A* **102** 062213
[41] Huang K Q, Zhao W L and Li Z 2021 *Phys. Rev. A* **104** 052405
[42] Zhao W L 2022 *Phys. Rev. Res.* **4** 023004
[43] Rossini D, Benenti G and Casati G 2006 *Phys. Rev. A* **74** 036209
[44] Bandyopadhyay J N 2009 *Europhys. Lett.* **85** 50006
[45] Adachi S, Toda M and Ikeda K 1988 *Phys. Rev. Lett.* **61** 659
[46] Graham R and Kolovsky A R 1966 *Phys. Lett. A.* **222** 47
[47] Park H K and Kim S W 2003 *Phys. Rev. A* **67** 060102
[48] Zhao W L and Jie Q L 2009 *Commun. Theor. Phys.* **51** 465
[49] Zhao W L, Jie Q L and Zhou B 2010 *Commun. Theor. Phys.* **54** 247
[50] Zhao W L and Jie Q L 2020 *Chin. Phys. B* **29** 080302
[51] Gadway B, Reeves J, Krinner L and Schneble D 2013 *Phys. Rev. Lett.* **110** 190401
[52] Rozenbaum E B and Galitski V 2017 *Phys. Rev. B* **95** 064303
[53] Wang W G, He L and Gong J 2012 *Phys. Rev. Lett.* **108** 070403
[54] Wang W G 2020 *Phys. Rev. E* **102** 012127
[55] Breuer H, Laine E and Piilo J 2009 *Phys. Rev. Lett.* **103** 210401
[56] Toikka L A and Andreanov A 2019 arXiv:1901.09362v1 [cond-mat.mes-hall]
[57] Smith A, Knolle J, Moessner R and Kovrizhin D L 2019 *Phys. Rev. Lett.* **123** 086602
[58] McGinley M, Nunnenkamp A and Knolle J 2019 *Phys. Rev. Lett.* **122** 020603
[59] Roy N and Sharma A 2021 *J. Phys.: Condens. Matter.* **33** 334001
[60] Yoshida B and Yao N Y 2019 *Phys. Rev. X* **9** 011006
[61] Harrow A W, Kong L, Liu Z W, Mehraban S and Shor P W 2021 *PRX Quantum* **2** 020339
[62] Knap M 2018 *Phys. Rev. B* **98** 184416
[63] Sharma K K and Gerdt V P 2021 *Quantum Inform. Process.* **20** 195
[64] Styliaris G, Anand N and Zanardi P 2021 *Phys. Rev. Lett.* **126** 030601
[65] Zanardi P and Anand N 2021 *Phys. Rev. A* **103** 062214
[66] Bergamasco P D, Carlo G G and Rivas A M F 2019 *Phys. Rev. Res.* **1** 033044